

Modeling of frequency response of transformer winding with axial deformations

K.M. GAWRYLCZYK, S. BANASZAK

*Department of Electrotechnology and Diagnostics
West Pomeranian University of Technology
ul. Sikorskiego 37, 70-313 Szczecin, Poland
e-mail: kmg@zut.edu.pl*

(Received: 31.05.2013, revised: 19.08.2013)

Abstract: One of important methods used for diagnostics of a transformer's active part is Frequency Response Analysis (FRA). It allows to determine the mechanical condition of windings, their displacements, deformations and electric faults, as well as some problems with internal leads and connections, core and bushings. Still pending problem is interpretation of measurements results. One of approaches is application of computer modeling to simulate various failure modes and connected with them changes in FRA response. The paper presents two types of models, one based on lumped parameters with RLC elements, and one based on distributed parameters with TLM method. Both methods give similar results, comparable to real measurements of simulated coil.

Key words: diagnostics, transformer, winding, frequency response analysis – FRA, lumped parameters method, transmission line method

1. Introduction

The computer modeling is a very helpful tool in many fields of science and engineering. It allows to create many variants of simulated phenomena or test setup and therefore save time and costs related to creation of physical models. However, their application needs involving many details of real processes and dependencies. One of fields, where computer modeling is developing very fast and has found a real need of application, is modeling of frequency response (FR) of transformer windings. Despite the fact that the first study on frequency response analysis can be found in 1978 [5], measurements of FR on power transformers have been introduced into industrial practice approx. ten years ago as Frequency Response Analysis method (FRA). This method is used for detection of mechanical faults in windings and core of a transformer. At the current stage of its development the measuring technique has been standardized [1], however there are still many problems considering interpretation of test results. FRA is a strictly comparative method, which means that FR measured along frequency

(usually in the range from 20 Hz to 2 MHz) has to be compared either to previous results, or similar units, or another phases of given transformer. The best is the first option, nevertheless for old units there are no fingerprint data available. Two remaining options may lead to different measurement mistakes and the recorded data is influenced by transformers' constructional details [9].

Because of limitations mentioned above there is a wide field for introducing computer models. By simulating real object and faults of different types it is possible to improve further analysis of industrial test results, because the simulation may give information on how FR depends on faults inside the active part of transformer. However, preparation of a computer model giving the same response as a real transformer is very difficult, as it is imperfect due to used simplifications and limitations of numerical calculations [3].

There were many different approaches used in modeling of FR. At the beginning the electric network models were used [4]. The efficiency of these models depended on the number of elements used in the model: capacitances, inductances, resistances and magnetic couplings. To prepare model giving FR similar to even simple single winding it was necessary to use very complex network consisting of many RLC elements. It needed a lot of calculations and the effect still was not satisfactory. Another approach was to introduce finite elements (FEM) calculations, which allowed to find values of electric parameters in faster and more detailed way. Early FEM models [2] were constructed for entire discs, and not for individual wires of the winding. Today, it seems as most effective approach to prepare algorithms allowing to calculate frequency response directly from electrical values obtained on the base of 3D finite elements calculations. The final result is then obtained directly and it makes possible modeling of quite complex objects, however, this approach requires very strong computers, particularly for 3D computation [5, 7]. For these reasons authors focused on a mixed method. It consists of the analysis of the electromagnetic field of the windings with circular-cylindrical symmetry and therefore using 2D coordinate system, evaluation of RLC parameters of the single wires in a wide frequency range, and then applying these parameters in the network model. Two network models are developed, the first one basing on simple RLC modeling, the other one incorporates transmission line method (TLM) for modeling of single wires.

2. RLC model

The simplest approach to RLC modeling is based on creating network of lumped parameters. These parameters are calculated from simplified equations and are limited to relationships between closest elements [4]. The solution can be carried out with standard software for circuit simulations, eg. SPICE or Micro-Cap. The example of such model is given on Figure 1.

Preparation of such model was very cumbersome, and did not give satisfactory results. The model proposed by authors takes into consideration relationships between all turns in the winding. It is based on the schematic branch shown on Figure 2.

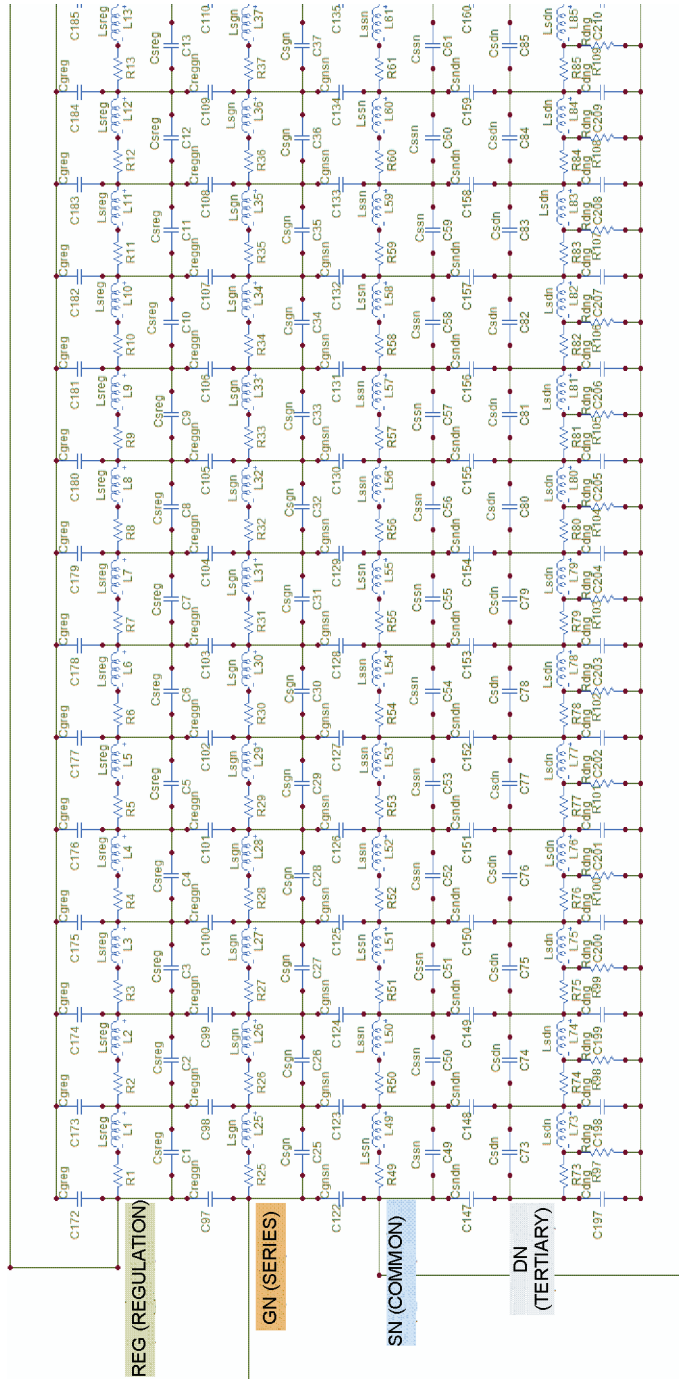


Fig. 1. Preparation of RLC-model of high-voltage winding of transformer

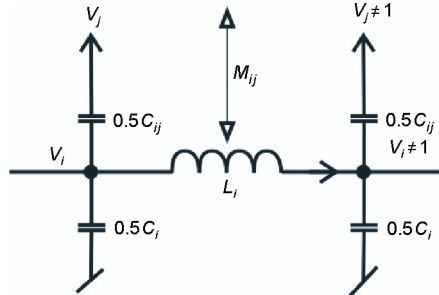


Fig. 2. Model of the single wire with interconnections to other wires

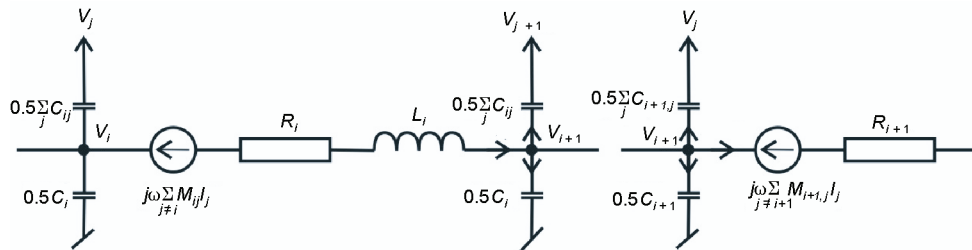


Fig. 3. Serial connection of two wires

Wires serial connection is shown in Figure 3. On this stage the algorithm does not allow parallel connections inside the winding. The proposed network model takes into account mutual inductances, as well as mutual capacitances between all wires, no matter how far apart.

For the model the following equations system is given:

$$\begin{aligned}
 I_i \cdot (R_i + j\omega L_i) &= V_i - V_{i+1} - j\omega \sum_{j \neq i} M_{ij} I_j, \\
 V_i - V_{i+1} &= I_i \cdot R_i + j\omega \sum_j M_{ij} I_j.
 \end{aligned}
 \tag{1}$$

The size of this equations system is $2 \times \text{number_of_turns}$ and its matrix is dense populated.

All RLC parameters are obtained from 2D analysis of electromagnetic field. Such approach allows more detailed calculations of field penetration into conducting wires by high frequency, than 3D modeling, because the number of finite elements may be much higher. Application of finite element method for the computation of lumped parameters seems still to be competitive versus analytical methods proposed in [6], which do not consider skin effect and proximity effect in the wires.

Both effects reduce the wires inductance about 10% at high frequency. Of course, application of 2D model results in some limitations coming from assumption that the winding is circular-symmetrical.

Calculation are done by commercial FEM package – ANSYS Maxwell. This program calculates impedance matrices used in RLC models. Self- and mutual capacitances determination is based on solving given electrostatic field equation:

$$\nabla \cdot (\varepsilon_r \varepsilon_0 \nabla \Phi(r, z)) = -\rho, \quad (2)$$

where: Φ is a scalar potential of electric field induced with charge having its density ρ , ε_0 and ε_r vacuum permittivity and relative environment permittivity.

To obtain self- and mutual inductances there was solved 2D electromagnetic field equation:

$$\nabla \times \frac{1}{\mu} (\nabla \times \mathbf{A}) + j \omega \gamma \mathbf{A} = \mathbf{J}_s, \quad (3)$$

where: \mathbf{A} is a magnetic vector potential, ω – supply current pulsation, μ and γ magnetic permeability of environment and its conductivity. \mathbf{J}_s is current density in windings. The induction values are obtained from magnetic field energy W_{AV} calculated from two models i and j with supply current having peak value I_{Peak} in given turns:

$$W_{AV} = \frac{1}{4} \int \mathbf{B}_i \cdot \mathbf{H}_j^* dV, \quad L_{ij} = \frac{4W_{AV}}{I_{Peak}^2} \int \mathbf{B}_i \cdot \mathbf{H}_j d\Omega, \quad (4)$$

\mathbf{B} and \mathbf{H} are vectors of induction and field intensity of magnetic field, having two spatial components in analyzed case. Self- and mutual capacitances have been obtained by energizing proper turns with voltage and calculating electric field energy W_{ij} :

$$W_{ij} = \frac{1}{2} \int_{\Omega} \mathbf{D}_i \cdot \mathbf{E}_j d\Omega, \quad C_{ij} = \frac{2W_{ij}}{V^2} \int_{\Omega} \mathbf{D}_i \cdot \mathbf{E}_j d\Omega, \quad (5)$$

\mathbf{D} and \mathbf{E} are vectors of electric induction and electric field intensity, having two components in analyzed case. Turns resistance values were received from active power losses P in them due to current flow having density \mathbf{J} :

$$P = \frac{1}{2\gamma} \int \mathbf{J} \cdot \mathbf{J}^* d\Omega, \quad R = \frac{2P}{I_{Peak}^2} = \frac{\int \mathbf{J} \cdot \mathbf{J}^* d\Omega}{\gamma I_{Peak}^2} = \frac{\int \mathbf{J} \cdot \mathbf{J}^* d\Omega}{\gamma}, \quad (6)$$

where: I_{Peak} is supply current peak value and γ – turn conductivity.

A very similar treatment of this problem may be found in [11]. The analyzed area was discretized with about 64k triangular elements. For better approximation at the boundary, the ballooning method is applied.

To illustrate skin- and proximity effects in the turns, the current density for one disc of the winding in Figure 4 is plotted.

3. Transmission line method – TLM

Distributed parameter networks were studied many years ago. Transmission line models are included in the most popular simulators, as SPICE. The history of transmission line models and model of AC motor may be found in [10].

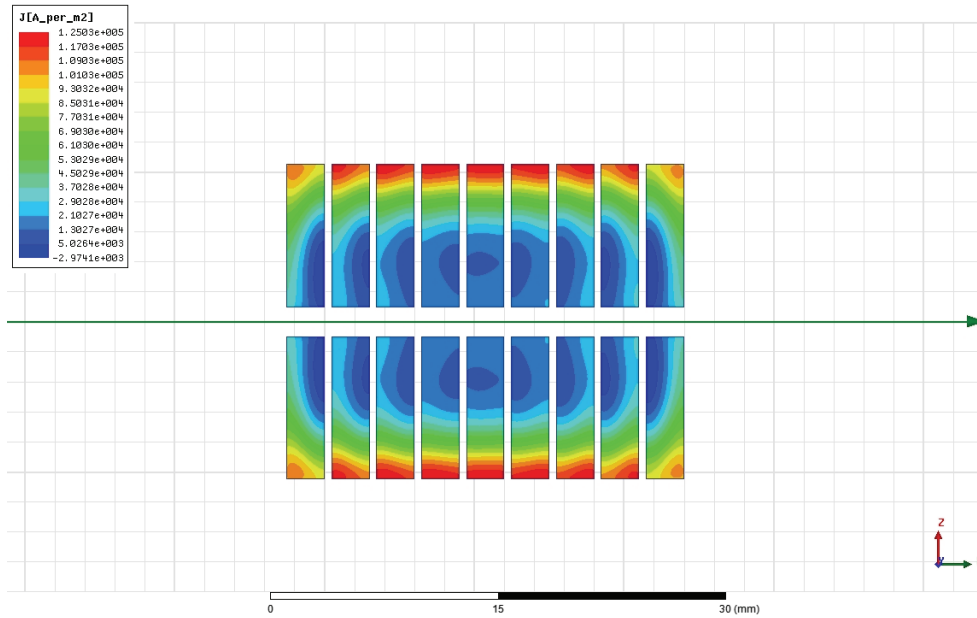


Fig. 4. Current density in one disc of the winding, frequency 1 kHz

Our work bases on the concept presented in [8]. Since the frequency of excitation current when using FRA reaches over 1 MHz and the length of primary winding of HV transformer is several hundred meters, it is comparable to wave length 300 m at the frequency of 1 MHz. From this reason good results may be obtained taking into consideration the wave effects.

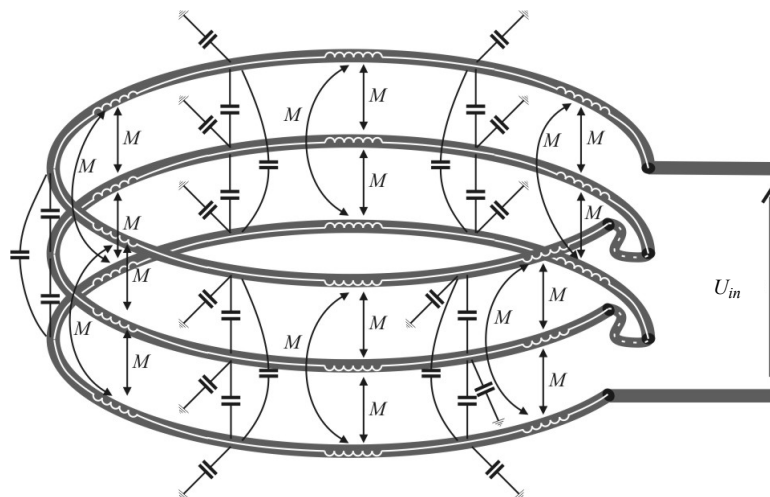


Fig. 5. Transmission line model of a simple winding

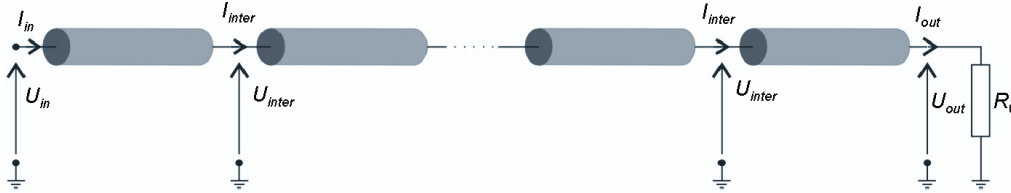


Fig. 6. Serial connection of wires modeled as transmission lines

Each turn from Figure 5 can be replaced by the element of transmission line. The turns are placed at one plane, what makes possible to use two dimensional models in finite element analysis. Currents and voltages are marked as in the following formulas:

$$\begin{aligned} \frac{d\mathbf{U}}{dx} &= -\mathbf{Z} \cdot \mathbf{I}, \quad \mathbf{Z} = \mathbf{R} + j\omega\mathbf{L} \left[\frac{\Omega}{\text{m}} \right], \\ \frac{d\mathbf{I}}{dx} &= -\mathbf{Y} \cdot \mathbf{U}, \quad \mathbf{Y} = j\omega\mathbf{C} \left[\frac{\text{S}}{\text{m}} \right]. \end{aligned} \quad (7)$$

\mathbf{Z} and \mathbf{Y} are matrixes of self and mutual impedances and admittances per unit of winding length x . Resistance matrix contains only self-resistances of turns. Equation (7) represent coupled differential equations, which are difficult to solve in presented form. Therefore matrixes \mathbf{Z} and \mathbf{Y} are decomposed to their diagonal form:

$$\mathbf{Z} = \mathbf{Q}_u \cdot \mathbf{Z}_d \cdot \mathbf{Q}_i^{-1}, \quad \mathbf{Y} = \mathbf{Q}_i \cdot \mathbf{Y}_d \cdot \mathbf{Q}_u^{-1}. \quad (8)$$

In the paper [8] it is proposed to obtain \mathbf{Q}_i from decomposition of $\mathbf{Z}\mathbf{Y}$ matrixes product, while \mathbf{Q}_u is determined as $\mathbf{Q}_u = \mathbf{Z} \cdot \mathbf{Q}_i$. In consequence there is always unitary matrix \mathbf{Z}_d , because $\mathbf{Z}_d = \mathbf{Q}_u^{-1} \cdot \mathbf{Z} \cdot \mathbf{Q}_i = [\mathbf{1}]$. Authors of this paper suggest to determine both matrixes, \mathbf{Q}_i and \mathbf{Q}_u , by eigendecomposition of:

$$\begin{aligned} \mathbf{Z} \cdot \mathbf{Y} &= \mathbf{Q}_u \cdot \mathbf{Z}_d \cdot \mathbf{Y}_d \cdot \mathbf{Q}_u^T, \\ \mathbf{Y} \cdot \mathbf{Z} &= \mathbf{Q}_i \cdot \mathbf{Y}_d \cdot \mathbf{Z}_d \cdot \mathbf{Q}_i^T. \end{aligned} \quad (9)$$

Matrixes \mathbf{Z} and \mathbf{Y} are symmetric. For their product it means $\mathbf{Z} \cdot \mathbf{Y} = (\mathbf{Y} \cdot \mathbf{Z})^T$. If the decomposition of $\mathbf{Y} \cdot \mathbf{Z}$ is known, the decomposition of $\mathbf{Z} \cdot \mathbf{Y}$ may be easily obtained from

$$\begin{aligned} \mathbf{Z} \cdot \mathbf{Y} &= (\mathbf{Y} \cdot \mathbf{Z})^T = (\mathbf{Q}_i \cdot \mathbf{Y}_d \cdot \mathbf{Z}_d \cdot \mathbf{Q}_i^{-1})^T = (\mathbf{Q}_i^{-1})^T \cdot \mathbf{Z}_d \cdot \mathbf{Y}_d \cdot \mathbf{Q}_i^T = \mathbf{Q}_u \cdot \mathbf{Z}_d \cdot \mathbf{Y}_d \cdot \mathbf{Q}_u^{-1} \\ \text{i.e. } \mathbf{Q}_u &= (\mathbf{Q}_i^{-1})^T \text{ and } \mathbf{Q}_i^{-1} = (\mathbf{Q}_i^T). \end{aligned} \quad (10)$$

In such case, for model without couplings between turns, its matrixes \mathbf{Z}_d and \mathbf{Y}_d are diagonal and do not change. Such decomposition allows to decouple telegraph equations.

$$\begin{aligned} \frac{d\mathbf{U}}{dx} &= -\mathbf{Q}_u \cdot \mathbf{Z}_d \cdot \mathbf{Q}_i^{-1} \cdot \mathbf{I} \rightarrow \mathbf{Q}_u^{-1} \cdot \frac{d\mathbf{U}}{dx} = \mathbf{Z}_d \cdot \mathbf{Q}_i^{-1} \cdot \mathbf{I} \rightarrow \frac{d\mathbf{U}_m}{dx} = -\mathbf{Z}_d \cdot \mathbf{I}_m, \\ \frac{d\mathbf{I}}{dx} &= -\mathbf{Q}_i \cdot \mathbf{Y}_d \cdot \mathbf{Q}_u^{-1} \cdot \mathbf{U} \rightarrow \mathbf{Q}_i^{-1} \cdot \frac{d\mathbf{I}}{dx} = -\mathbf{Y}_d \cdot \mathbf{Q}_u^{-1} \cdot \mathbf{U} \rightarrow \frac{d\mathbf{I}_m}{dx} = -\mathbf{Y}_d \cdot \mathbf{U}_m. \end{aligned} \quad (11)$$

From Equations (11) it can be seen that $\mathbf{U}_m = \mathbf{Q}_u^{-1} \mathbf{U}$, and $\mathbf{I}_m = \mathbf{Q}_i^{-1} \mathbf{I}$. The solution of these equations is carried out in known way leading to a chain matrix of single element k of a transmission line:

$$\mathbf{A}_{m,k} = \begin{bmatrix} ch\beta_k l & Z_{c,k} \cdot sh\beta_k l \\ \frac{1}{Z_{c,k}} sh\beta_k l & ch\beta_k l \end{bmatrix} = \begin{bmatrix} A_{m,uu,k} & A_{m,ui,k} \\ A_{m,iu,k} & A_{m,ii,k} \end{bmatrix} \quad (12)$$

where:

$$\beta_k = \sqrt{Z_{dk,k} \cdot Y_{dk,k}}, \quad Z_{c,k} = \sqrt{\frac{Z_{dk,k}}{Y_{dk,k}}}, \quad l - \text{length of a turn.}$$

Values of propagation coefficient β and wave impedance Z_c of each turn k are determined on the base of diagonal elements k,k of decomposed matrixes \mathbf{Z}_d and \mathbf{Y}_d . Single turns can be now joined together, to create winding:

$$\begin{bmatrix} \mathbf{U}_m \\ \mathbf{I}_m \end{bmatrix} = \begin{bmatrix} \mathbf{A}_{m,uu} & \mathbf{A}_{m,ui} \\ \mathbf{A}_{m,iu} & \mathbf{A}_{m,ii} \end{bmatrix} \begin{bmatrix} \mathbf{U}_m(0) \\ \mathbf{I}_m(0) \end{bmatrix}, \quad (13)$$

where $\mathbf{A}_{m,xx}$ are diagonal matrixes containing necessary elements taken from the matrix of single elements (12). $\mathbf{U}_m(0)$ and $\mathbf{I}_m(0)$ are values at the beginning of turns. When replacing decomposed voltages and currents by their original values, it is obtained:

$$\begin{bmatrix} \mathbf{Q}_u^{-1} \cdot \mathbf{U} \\ \mathbf{Q}_i^{-1} \cdot \mathbf{I} \end{bmatrix} = \begin{bmatrix} \mathbf{A}_{m,uu} & \mathbf{A}_{m,ui} \\ \mathbf{A}_{m,iu} & \mathbf{A}_{m,ii} \end{bmatrix} \begin{bmatrix} \mathbf{Q}_u^{-1} \cdot \mathbf{U}(0) \\ \mathbf{Q}_i^{-1} \cdot \mathbf{I}(0) \end{bmatrix}, \quad (14)$$

and following system of equations for the whole winding:

$$\begin{bmatrix} \mathbf{U} \\ \mathbf{I} \end{bmatrix} = \begin{bmatrix} \mathbf{Q}_u \cdot \mathbf{A}_{m,uu} \cdot \mathbf{Q}_u^{-1} & \mathbf{Q}_u \cdot \mathbf{A}_{m,ui} \cdot \mathbf{Q}_i^{-1} \\ \mathbf{Q}_i \cdot \mathbf{A}_{m,iu} \cdot \mathbf{Q}_u^{-1} & \mathbf{Q}_i \cdot \mathbf{A}_{m,ii} \cdot \mathbf{Q}_i^{-1} \end{bmatrix} \begin{bmatrix} \mathbf{U}(0) \\ \mathbf{I}(0) \end{bmatrix}, \quad (15)$$

which can be simplified to:

$$\begin{bmatrix} \mathbf{U} \\ \mathbf{I} \end{bmatrix} = \begin{bmatrix} \mathbf{A}_{uu} & \mathbf{A}_{ui} \\ \mathbf{A}_{iu} & \mathbf{A}_{ii} \end{bmatrix} \begin{bmatrix} \mathbf{U}(0) \\ \mathbf{I}(0) \end{bmatrix}. \quad (16)$$

According to indicators introduced on Figure 6, vectors of voltages and currents contain components presented in Equation (17). To calculate transfer function of the winding, it is not necessary to know voltage $\mathbf{U}_{\text{inter}}$ and current $\mathbf{I}_{\text{inter}}$ vectors inside the winding, as well as current

I_{out} . All is needed are values of voltages U_{in} and U_{out} .

$$\begin{bmatrix} U_{in} \\ \mathbf{U}_{inter} \\ I_{in} \\ \mathbf{I}_{inter} \end{bmatrix} = \begin{bmatrix} \mathbf{A}_{uu} & \mathbf{A}_{ui} \\ \mathbf{A}_{iu} & \mathbf{A}_{ii} \end{bmatrix} \begin{bmatrix} \mathbf{U}_{inter} \\ U_{out} \\ \mathbf{I}_{inter} \\ I_{out} \end{bmatrix} = \begin{bmatrix} \mathbf{A}_{uu} & \mathbf{A}_{ui} \\ \mathbf{A}_{iu} & \mathbf{A}_{ii} \end{bmatrix} \begin{bmatrix} \mathbf{U}_{inter} \\ U_{out} \\ \mathbf{I}_{inter} \\ \frac{U_{out}}{R_0} \end{bmatrix} \quad (17)$$

It was assumed that supply voltage is $U_{in} = 1V$. To determine voltages, system of equations is converted to form presented on Figure 7b:

$$\begin{bmatrix} U_{in} \\ \mathbf{U}_{inter} \\ I_{in} \\ \mathbf{I}_{inter} \end{bmatrix} = \begin{bmatrix} \mathbf{A}_{uu,1} & A_{uu,1,n} & \mathbf{A}_{ui,1} & A_{ui,1,n} \\ \hat{\mathbf{A}}_{uu} & \mathbf{A}_{uu,n} & \hat{\mathbf{A}}_{ui} & \mathbf{A}_{ui,n} \\ \mathbf{A}_{iu,1} & A_{iu,1,n} & \mathbf{A}_{ii,1} & A_{ii,1,n} \\ \hat{\mathbf{A}}_{iu} & \mathbf{A}_{iu,n} & \hat{\mathbf{A}}_{ii} & \mathbf{A}_{ii,n} \end{bmatrix} \begin{bmatrix} \mathbf{U}_{inter} \\ U_{out} \\ \mathbf{I}_{inter} \\ \frac{U_{out}}{R_0} \end{bmatrix} \quad (18)$$

and finally to (19), which gives necessary value of U_{out} :

$$\begin{bmatrix} U_{in} \\ \mathbf{U}_{inter} \\ I_{in} \\ \mathbf{I}_{inter} \end{bmatrix} = \begin{bmatrix} \mathbf{A}_{uu,1} & A_{uu,1,n} + \frac{A_{ui,1,n}}{R_0} & \mathbf{A}_{ui,1} & 0 \\ \hat{\mathbf{A}}_{uu} - 1 & \mathbf{A}_{uu,n} + \frac{\mathbf{A}_{ui,n}}{R_0} & \hat{\mathbf{A}}_{ui} & 0 \\ \mathbf{A}_{iu,1} & A_{iu,1,n} + \frac{A_{ii,1,n}}{R_0} & \mathbf{A}_{ii,1} & -1 \\ \hat{\mathbf{A}}_{iu} & \mathbf{A}_{iu,n} + \frac{\mathbf{A}_{ii,n}}{R_0} & \hat{\mathbf{A}}_{ii} - 1 & 0 \end{bmatrix} \begin{bmatrix} \mathbf{U}_{inter} \\ U_{out} \\ \mathbf{I}_{inter} \\ I_{in} \end{bmatrix} \quad (19)$$

Figure 7a presents matrixes and vectors from Equation (17), while Figure 7b shows corresponding structure used in Equations (18) and (19).

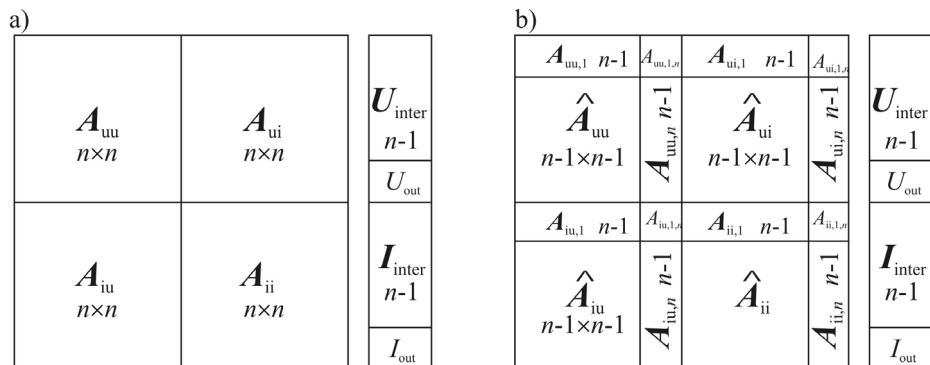


Fig. 7. Structure of the matrices in Equations system (17) and (18), (19)

4. Comparison of simulation results to measurement

In order to evaluate proposed models a practical measurement experiment has been performed. A part of a real transformer winding was used for FR measurements, at the beginning in 'healthy' condition (baseline measurement), then after introducing forced deformations. Because of the axial symmetry of the model, only axial deformations were considered. They were based on changing the gap between discs. There were performed several versions of deformation measurements and corresponding models, one of them is discussed below. All of them gave similar conformity of measurement and simulation results. Fig. 8 shows the view of winding used in the experiment. All measurements were taken with commercial device FRAnalyzer from Omicron.



Fig. 8. The winding under investigation with introduced axial shift

The first step was to compare FR of the winding coming from the measurement and the model in a 'healthy' state. It can be seen on Figures 8 and 9 – respectively a module and a phase shift of transfer function. Both models – RLC and TLM – show good conformity in the whole frequency range. Slight differences are in the shift along the frequency starting on the main resonance at $4 \cdot 10^5$ to $5 \cdot 10^6$, and in the damping in the same range. Possible source of this inaccuracy is in imperfection of test object, because the discs of the winding might have been placed asymmetrically and there is also influence of surrounding environment on e.g. capacitances. Nevertheless all resonances are represented in model's FR.

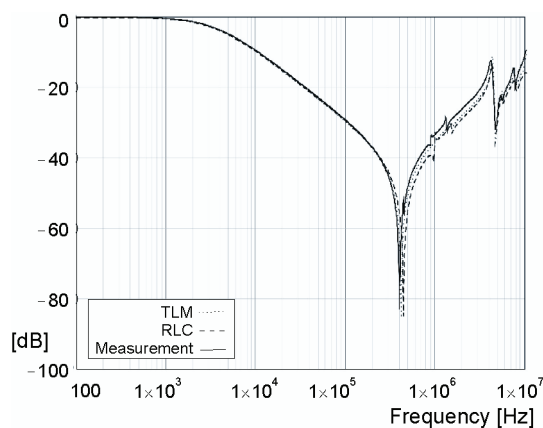


Fig. 9. Comparison of results before deformation of winding (module of transfer function)

Fig. 10. Comparison of results before deformation of winding (phase shift of transfer function)

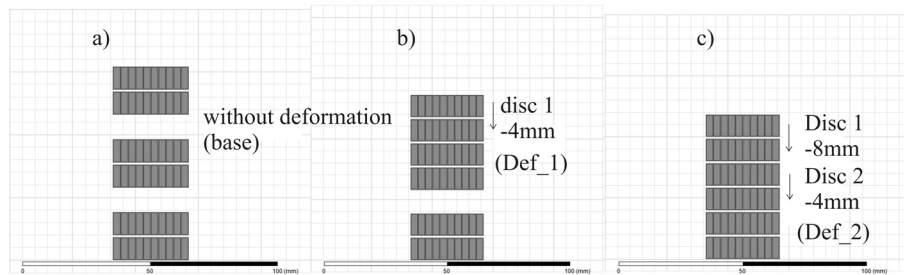
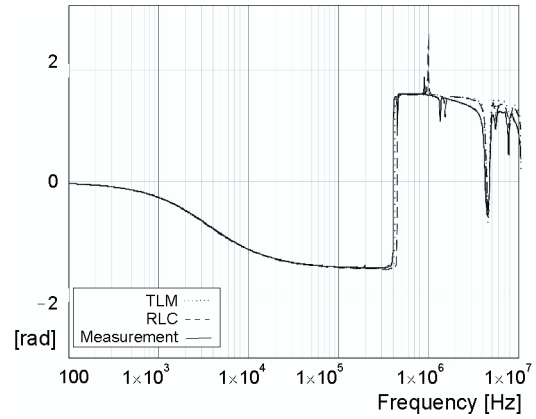
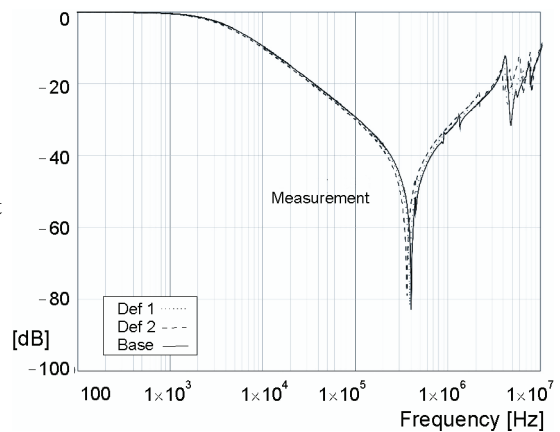


Fig. 11. Introduced axial displacements of the winding: a) base, b) Def 1, c) Def 2

In the next step two deformations were introduced according to Figure 11. The impact of a deformation on the measurement is presented on Figure 12.

Fig. 12. Sensitivity to axial shift – measurement (module of transfer function)



The main resonance is shifted to lower frequency, the shape of small resonances on capacitive slope approx. 1 MHz is also affected, as well as the whole region above 500 MHz. Similar effect is observed in the case of both models, presented on Figure 13 – RLC and

Figure 14 – TLM. The kind and direction of shape changes are the same if compared to measurement, only the scale differs. This might be the result of factors mentioned above – asymmetry of the real object and the influence of test environment.

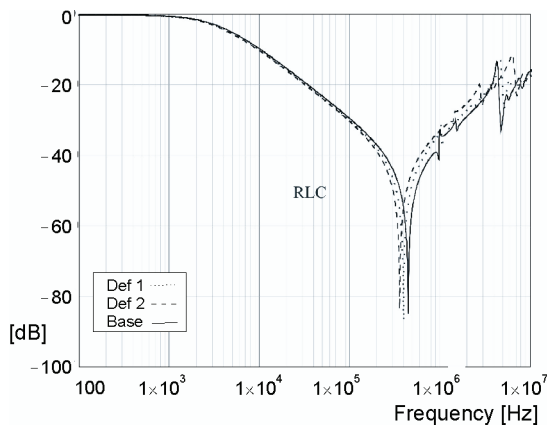


Fig. 13. Sensitivity to axial shift – RLC model (module of transfer function)

From comparison of measurement results to RLC and TLM simulations it can be concluded that both methods give good conformity to real phenomena. In industrial power transformers important range of FR is placed in lower frequencies – deformations usually influence a frequency range from 10 kHz to 500 kHz, which makes the problem easier for further modeling. Presented models worked properly even to 10 MHz.

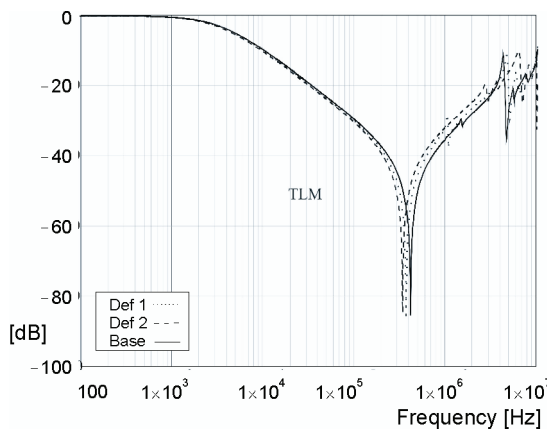


Fig. 14. Sensitivity to axial shift – TLM model (module of transfer function)

5. Conclusions

Results shown in the paper were obtained for the winding removed from the core. Because the presence of the core by high supplying frequency has no influence on windings' parameters, we expect similar results when taking into account magnetic parts. Our model was

limited to 60 wires, which is only the part of a real winding. It has been caused by the calculating capabilities of the Maxwell package concerning evaluation of impedance matrix.

Both presented methods, RLC and TLM modeling, deliver comparable results. Observing the phase shift of transfer function slightly better exactness of TLM method in high frequency range can be remarked.

The described methods can be applied to the analysis of transformers with a large number of turns. In this case we expect difficulties in determining capacitances and inductances of the wires using commercial packages. In many cases, the circular-cylindrical symmetry allowing for 2D analysis can be used. However, since the aim of future work is to analyze the deformation of the windings, it will need the full 3D field analysis.

Practical application of these models would allow preparation of tools simulating various failures in transformer's active part and their influence on FRA curve. By obtaining models giving response very close to the real measurement it would be possible to perform such simulations for many constructions of transformers, in various connection set-ups and therefore prepare a lot of data for automated assessment tools, e.g. neural networks.

Acknowledgment

Presented results are part of research project no. N N510 698240 entitled "Algorithm for identification of transformers windings deformations on the base of frequency response measurements (FRA)", financed by Polish National Science Center.

References

- [1] *International standard IEC 60076-18 Power transformers – Part 18. Measurement of frequency response* (2012).
- [2] Azzouz Z., Foggia A., Pierrat L., Meunier G., *3d Finite Element Computation of the High Frequency Parameter of Power Transformer Windings*. IEEE Trans. on Magnetics 29(2): 1407-1410 (1993).
- [3] Banaszak Sz. *Conformity of Models and Measurements of Windings Deformations in Frequency Response Analysis Method*. Przegląd Elektrotechniczny 7: 278-280 (2010).
- [4] Bjerkan E., *High Frequency Modeling of Power Transformers. Stresses and Diagnostics*. Doctoral Thesis, Norwegian University of Science and Technology (2005).
- [5] Dick E.P., Erven C.C., *Transformer Diagnostic Testing by Frequency Response Analysis*, IEEE Trans. on Power Apparatus and Systems PAS-97, 6: 2144-2153 (1978).
- [6] Eslamian M., Vahidi B., *New Methods for Computation of the Inductance Matrix of Transformer Windings for Very Fast Transients Studies*. IEEE Trans. on Power Delivery 27(4): 2326-2333 (2012).
- [7] Gawrylczyk K.M., Banaszak Sz., *Computer Modeling in the Diagnostics of Transformers' Windings Deformations*. Computer Application in Electrical Engineering, Poznań University of Technology, pp. 132-140 (2010).
- [8] de Gerssem H., Henze O., Weiland T., Binder A. *Simulation of Wave Propagation Effects in Machine Windings*, COMPEL 29(1): 23-38 (2010).
- [9] Jayasinghe J.A.S.B, Wang Z.D., Darwin A.W., Jarman P.N., *Practical Issues in Making FRA Measurements on Power Transformers*, XIVth International Symposium on High Voltage Engineering, Beijing, China, G-013 (2005).
- [10] Skibinski G., Kerkman R., Leggate D., Pankau J., Schlegel D., *Reflected Wave Modeling Techniques for PWM AC Motor Drives*, Proc. of the IEEE Applied Power Conference, Anaheim, CA, USA, pp. 1021-1029.
- [11] Wang H., Butler K.L., *Finite Element Analysis of Internal Winding Faults in Distribution Transformers*, IEEE Trans. on Power Delivery 16(3): 422-427 (2001).